ON THE DELAMINATION OF MULTIDIRECTIONAL LAMINATES UNDER MODE I LOADING

N. Blanco[1*], T. A. Sebaey[1,2], J. Costa[1], C. S. Lopes[3]

[1]*Advanced Materials and Analysis for the Structural Design (AMADE), Polytechnic School, Universitat de Girona, Campus Montilivi s/n, 17071 Girona, Spain*
[2]*Mechanical Design and Production Dept., Faculty of Engineering, Zagazig University, B.O. Box 44519, Zagazig, Sharkia, Egypt*
[3]*Madrid Institute for Advanced Studies of Materials (IMDEA-Materiales), Profesor Aranguren s/n, 28040 Madrid, Spain*
**norbert.blanco@udg.edu*

Keywords: delamination, multidirectional laminate, fracture toughness, mode I.

Abstract
The experimental characterization of the mode I interlaminar fracture toughness of multidirectional composite laminates is complicated because the crack tends to migrate from the propagation plane (crack jumping) invalidating the tests. However, the selection of the appropriate bending stiffness of the beam arms can avoid this tendency allowing this characterization. In the present work, six stacking sequences numerically analyzed have been experimentally tested to validate the methodology. The obtained results show that crack jumping can be effectively avoided by increasing the stiffness of the crack arms. Micrographies of the tested specimens show that the delamination is not a perfect interlaminar fracture as fiber tearing is also involved. The obtained toughness values show a dependency upon both the amount of fiber bridging and the interface angles.

1 Introduction

Delamination is considered as one of the most critical failure modes in laminated composites and it is usually characterized using unidirectional specimens to avoid the difficulties associated with measuring it in multidirectional laminates. Basically, extradamage mechanisms such as crack jumping and double cracking invalidate the interlaminar fracture toughness characterization. Different attempts to avoid crack jumping have been reported in the literature such as two modifications of the DCB specimen, the predelaminated edge specimen [1] and the side grooved specimen [2], and an asymmetric DCB specimen [3]. However, none of these has proven to be always successful in overcoming the problem.

A numerical study to avoid crack jumping in multidirectional laminates was presented in an earlier study [4]. The matrix cracking failure index, calculated based on LaRC04, was considered as an indicator of crack jumping i.e. the higher the matrix cracking failure index the higher the tendency to crack jumping. The paper concluded that crack jumping could be avoided by increasing the bending stiffness of the crack beam arms. The current work corresponds to the experimental validation of that specimen design. Six multidirectional configurations have been checked for crack jumping under mode I loading. The crack propagation process was monitored using a traveling microscope. To obtain the fracture toughness, the Modified Compliance Calibration (MCC) data reduction scheme was used only for those specimens where the crack propagation had been purely interlaminar (with no crack jumping). In some cases, it was impossible to recognize if there was crack jumping or not, based on the traveling microscope images due to the high amount of fiber bridging. Consequently, parts of the specimen were cut within the propagation areas and the edges of these parts were checked using an optical microscope.

2 Materials and testing methods

2.1 Material and specimen configurations

The material used in this work was the unidirectional carbon/epoxy Hexcel AS4/8552. The preimpregnated plies were laid in the desired configuration and cured according to the specifications provided by Hexcel. After curing, the specimens were cut into the desired dimensions using a diamond disc. The measured mechanical properties of the unidirectional AS4/8552 are listed in Table 1.

Elastic properties	E_{11} = 129.0 GPa; E_{22} = 7.6 GPa; G_{12} = 5.03 GPa; ν_{12} = 0.32
Strength	X^T = 2240 MPa; Y^T = 26 MPa; S^L = 83.78 MPa
Fracture toughness	G_{Ic} = 244 J/m^2; G_{IIc} = 780 J/m^2
Ply thickness	t = 0.125 mm

Table 1. Elastic and mechanical properties of the unidirectional Hexcel AS4/8552 plies.

Table 2 summarizes the tested stacking sequences and their specifications (NL refers to the number of layers, θ_1 and θ_2 are the orientations of the two layers at the delamination plane and FI_{MT} is the matrix cracking failure index predicted numerically). According to the numerical simulations reported, the first four configurations are not expected to have crack jumping while this phenomenon is expected to occur in the last two. All the configurations except the second and sixth are standard DCB specimens in which the two crack arms have the same stiffness. Configurations two and six present a small difference in the bending stiffness between the two arms resulting in asymmetric DCB specimens and some mode II contribution might be expected during the tests. However, it has been numerically checked and this contribution is less than 4%.

Laminate	Stacking sequence	NL	$\theta_1//\theta_2$	FI_{MT}
S2_20_30_-30	$[(30/-30/0_8)_s//(-30/30/0_8)_s]$	40	30//-30	0.2
S2_20_0_30	$[0_{20}//(30/-30/0_8)_s]$	40	0//30	0.5
S2_20_45_-45	$[(45/-45/0_8)_s//(-45/45/0_8)_s]$	40	45//-45	0.5
S4_12_45_-45	$[(45/-45/0_4)_s//(-45/45/0_4)_s]$	24	45//-45	0.7
S1_12_45_-45	$[(45/-45/90/\pm45/0)_s//(-45/45/90/\pm45/0)_s]$	24	45//-45	1.0
S1_12_15_-75	$[(15/-15/90/\pm45/0)_s//(-75/75/90/\pm45/0)_s]$	24	15//-75	2.5

Table 2. Configuration of the tested specimens and their characteristics (// indicates the delamination plane).

2.2 Delamination tests

The geometry of the specimens used was compliant with the ISO 15024 standard. The thickness of the specimens varied depending on the configuration (see Table 2). The Side Clamped Beam (SCB) hinge clamping system, developed by Renart et al. [5], was used to load the specimen. Five test specimens were tested per configuration. During the propagation process, the crack front was observed and the propagation process was recorded using an optical system composed of a high-resolution video camera (JVC TK-1270) and a long distance microscope (Questar QM 100 MK III). For a better understanding of the fracture process, for each configuration a 25 x 10 mm part of ne specimen was cut after the test and its edge was observed using a fluorescence optical microscope (Leica, DMR-XA) to inspect the path followed by the crack during propagation.

2.3 Data reduction procedure

The standard data reduction schemes, developed for unidirectional laminates, are usually used in multidirectional specimens. Gong et al. [6] presented a comparison between the different data reduction schemes and concluded all of them led to similar results in multidirectional specimens except for the simple beam theory. For the current work the Modified Compliance Calibration (MCC) reduction scheme was used to calculate the energy release rate, G_{Ic}, as:

$$G_{Ic} = \frac{3m}{4h}\left(\frac{P}{b}\right)^2 \left(\frac{bC}{N}\right)^{\frac{2}{3}} \quad (1)$$

where h is the thickness of one arm, b is the specimen width, P is the applied load, C is the load line compliance, m is the slope of $(bC/N)^{1/3}$ vs. the delamination length normalized by the specimen thickness ($a/2h$) and N is the load block correction factor. With respect to the two ADCB specimens, the mode II contribution is below 4% and, consequently, this contribution was neglected and Eq. (1) was used.

3 Results and discussion

3.1 Crack propagation

Fig. 1 shows examples of the obtained crack propagation modes: smooth propagation, stair-shape propagation, crack jumping and double cracking. For some configurations only one propagation mode was found, while for others different propagation modes were observed in different specimens. The number of specimens corresponding to each propagation mode for each configuration is summarized in Table 3. The modes included in Table 3 correspond to the first detected propagation mode. In most of the cases, where crack jumping is observed, it occurs when extending the initial crack from the insert (during the precracking).

Laminate	Smooth propagation	Stair-shape	Jumping	Double cracking
S2_20_30_-30	5	-	-	-
S2_20_0_30	2	-	2	1
S2_20_45_-45	5	-	-	-
S4_12_45_-45	3	1	-	1
S1_12_45_-45	2	3	-	-
S1_12_15_-75	-	-	5	-

Table 3. Number of specimens corresponding to each failure mode.

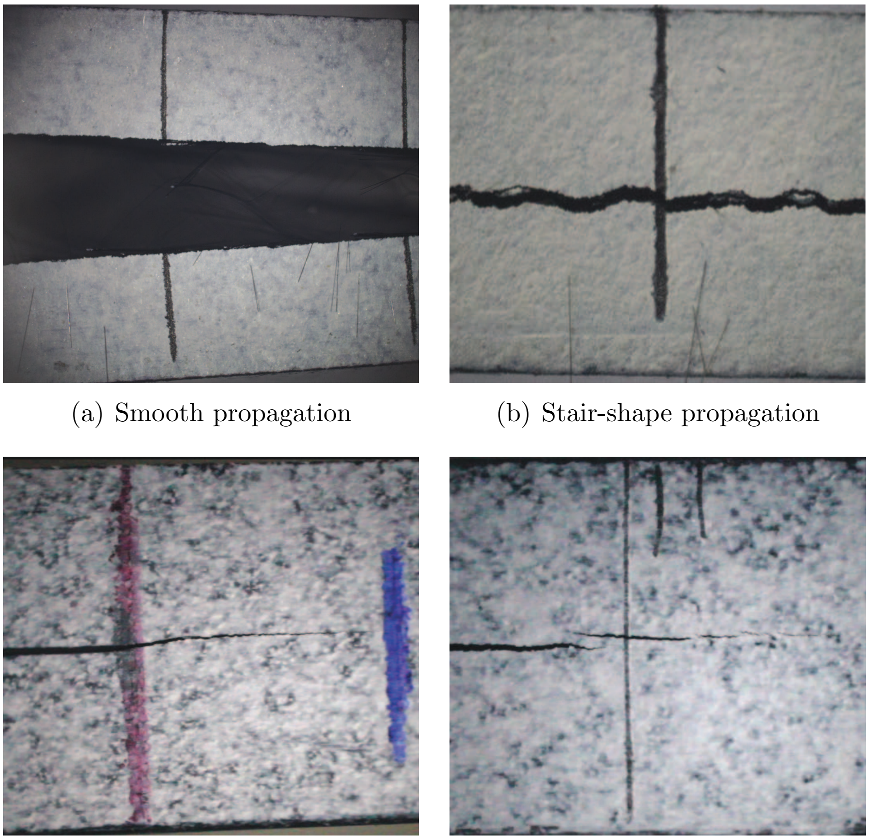

(a) Smooth propagation (b) Stair-shape propagation

(c) Crack jumping (d) Double cracking

Figure 1. Different delamination propagation modes in multidirectional laminates under mode I loading.

As mentioned earlier, five test specimens are tested for each configuration. In general, the lower the value of the matrix cracking failure index, Table 2, the higher the number of valid specimens (specimens at which the crack advances in smooth propagation mode), Table 3. However the configuration S2_20_0_30 is an exception to this trend. For this configuration, the crack either jumps to the 30/-30º interface in two specimens, or in one case a second crack initiates at this interface spontaneously creating the phenomenon of double cracking. It should be noted that, due to its high ply mismatch angle (60º), the 30/-30º interface develops considerable interlaminar shear stresses as the arm bends, hence its propensity to delaminate even without a triggering intraply matrix crack.

Some images of the crack propagation path on the edge of the specimen obtained by composing different specimen micrographs can be observed in Fig. 2. As shown in the figure, the use of the optical microscope can reveal interesting details of the crack propagation in multidirectional laminates. The first and the second images, Fig. 2(a) and Fig. 2(b), show examples of the smooth crack propagation in the original interface plane. Fig. 2(c) shows the resulting crack profile when crack jumping occurs. It can be observed how the crack has changed its propagation plane several times involving transverse matrix cracking and fiber breakage. Fig. 2(d) shows one specimen where double cracking has occurred.

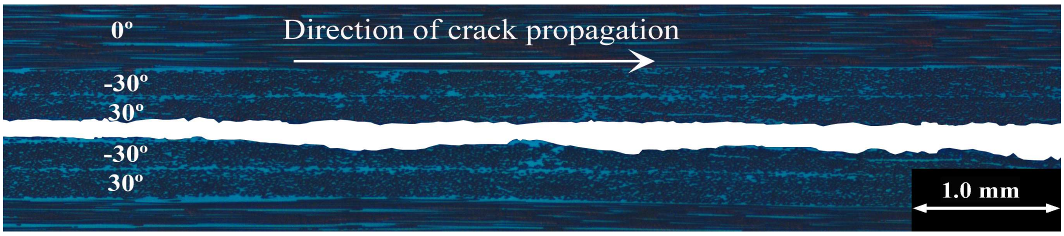

(a) Specimen S2_20_30_-30, 20 mm away from the inset tip

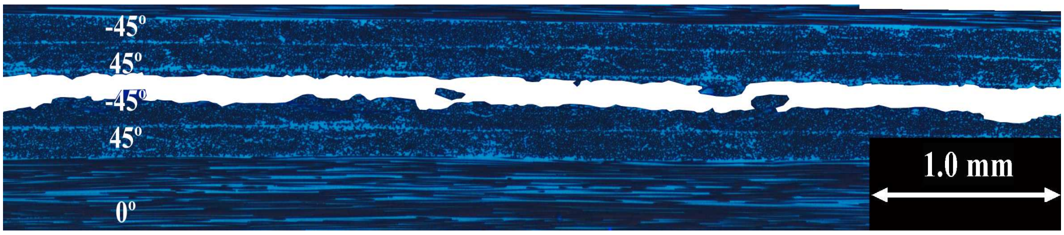

(b) S4_12_45_-45, 5 mm away from the insert tip

(c) S1_12_15_-75, at the insert tip

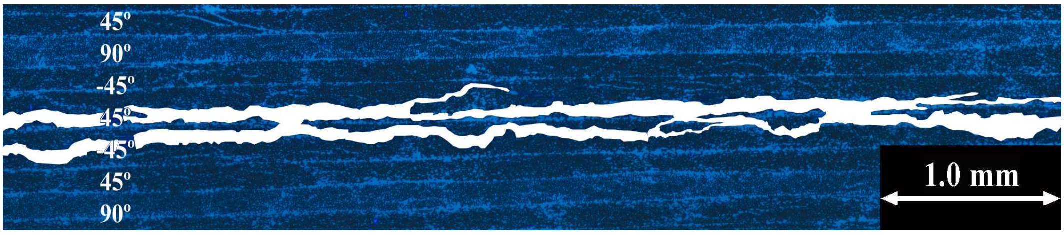

(d) S1_12_45_-45, 20 mm away from the insert tip

Figure 2. Propagation mode in multidirectional laminates.

Fig. 3 shows a more detailed view of one specimen where crack jumping is not observed. The three images are taken at different positions along the crack. The first image, Fig. 3(a), corresponds to the well-known delamination phenomenon. The second, Fig 3(b), corresponds to the propagation of the crack near to the middle of one layer. The third image, Fig. 3(c), shows crack propagation in one of the two plies surrounding the insert plane, but close to the interface. According to the ASTM D5573, this mechanism can be identified as light fiber tearing. As a general trend for all the configurations, the delamination starts by pure interlaminar fracture, Fig. 3(a) and after that, any of the three mechanisms can appear. The most common failure mechanism is the light fiber tearing.

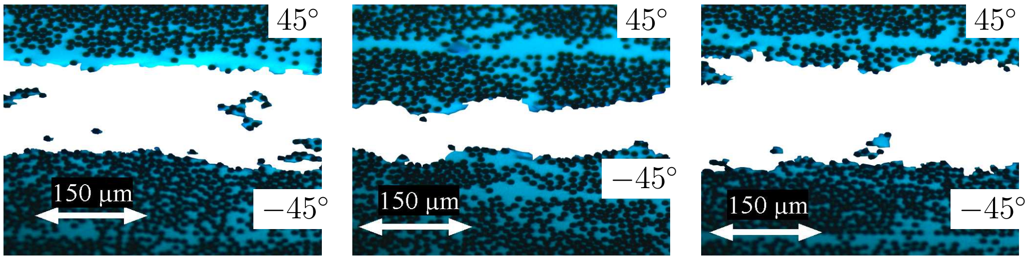

(a) Interlaminar (b) Intralaminar (c) Light fiber tearing

Figure 3. Delamination mechanisms for S4_12_45_-45.

3.2 Fracture toughness

Table 4 summarizes the initiation and propagation fracture toughness values, and the corresponding Coefficient of Variation (CV), for each configuration. Only the specimens that did not show crack jumping, Table 3, are considered in the calculations. For the configuration S1_12_15_-75, both the onset and propagation fracture toughness values are not calculated because crack jumping is observed in all the specimens. Considering that, usually, the crack initiates near the specimen mid-width, the nonlinear (NL) point is the most meaningful when measuring onset fracture toughness [6]. The nonlinear points for different configuration are summarized in Table 4.

	Onset (NL point)		Propagation	
Laminate	**Mean (J/m^2)**	**CV (%)**	**Mean (J/m^2)**	**CV (%)**
S2_20_30_-30	195.7	10.1	341.4	3.5
S2_20_0_30	194.3	0.2	315.7	2.6
S2_20_45_-45	203.8	8.1	405.3	8.0
S4_12_45_-45	185.9	2.7	490.6	9.3
S1_12_45_-45	205.0	8.1	593.5	0.9
S1_12_15_-75	-	-	5	-

Table 4. Experimentally measured onset and propagation values of mode I fracture toughness.

The onset fracture toughness is similar for all the configurations and interface angles with less than 5% coefficient of variation. This result is reasonable because, at the insert tip, the effect of the interface angles is insignificant due to the existence of a resin rich area in front of the insert tip. Moreover, fiber bridging does not affect the onset process and, at the initiation point, the crack front is straight and perpendicular to the crack front advance direction (hence, the crack front shape effect also vanishes). With respect to the propagation fracture toughness data, it can be noted that the toughness of the multidirectional interfaces is higher than that of the unidirectional ones (see Table 1 and Table 4). The same result was found by other researchers [7,8]. The interface 0//30º has the lower value of toughness while the interface 45//-45º yields the maximum value of the fracture toughness when tested with high flexible beam arms.

For the interface 45◦//-45◦, it is noted that the toughness value is a function of the specimen stacking sequence. Shokrieh and Heidari-Rarani [9] recorded a similar deviation in the fracture toughness measured for 0◦//0◦ interface using different stacking sequences in the beam arms. The higher the flexibility of the beam arms the tougher the material. The reason behind this response is the amount of fiber bridging. Different amounts of fiber bridging are recognized, for different configurations, during propagation. A comparison between the amount of fiber bridging for the interface 45//-45º with different stacking sequence is made in

Fig. 4. It is clear that the higher the flexibility of the arms, the higher the amount of fiber bridging for the same ply interface. This fact justifies the difference in the measured fracture toughness for the three different specimen configurations with 45//-45º interface reported in Table 4. This is in agreement with the results found in Ref. [10–12].

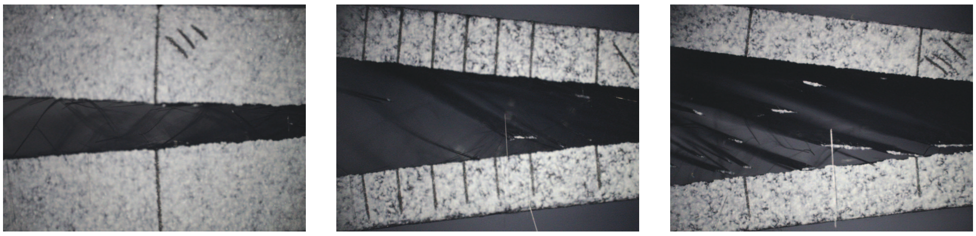

(a) S2_20_45_-45 (b) S4_12_45_-45 (c) S1_12_45_-45

Figure 4. Fiber bridging for interface 45//-45º measured using different stacking sequences.

The comparison between the propagation toughness data of the configurations S2_20_45_-45, S4_12_45_-45 and S1_12_45_-45 shows that the effect of fiber bridging on the fracture toughness for the same interface angle is 47%. On the other hand, the comparison between the data of the configurations S2_20_30_-30, S2_20_0_30 and S2_20_45_-45 shows that the effect of the interface angle is 29%, at almost the same bending stiffness. This indicates that fiber bridging effect is higher than the mismatch angle effect.

In Section 3.1, it has been demonstrated that the smooth crack propagation mostly occurs between a composite layer and a resin rich area or inside one layer close to the interface (light fibre tearing mode). The fact that the crack propagates inside a layer and not at the interface between two layers might indicate that the measured fracture toughness depends more on the angle between the crack growth direction and the ply orientation in which the crack propagates, than on the mismatch angles of the plies adjacent to the interface. In fact, when comparing two cases in which the crack propagated inside the 30º layer (S2_20_30_-30 and S2_20_0_30) the measured difference in fracture toughness is only 9%. And these values differ up to 30% from that of the batch S2_20_45_-45, where the crack propagates inside the 45º layer. However, further investigation should be carried out to support this idea. From a practical point of view, the presented data indicate that the current engineering practice of assuming that the fracture toughness at any interface of a composite structure corresponds to the results of tests in UD plies (0//0º specimens), underestimates it. Moreover, nowadays it is a common practice in composites design to analyze the effect of delaminations by using cohesive finite elements based on 0//0º interlaminar fracture toughness values resulting in save but inaccurate predictions. A truly optimized design requires taking into account the dependence on the interface angle and on the crack orientation with respect to the ply angles.

4 Conclusions

Delamination tests in mode I were conducted to validate the numerical study performed by the authors and presented in [4]. Six multidirectional configurations were defined by means of numerical design and tested experimentally to check the possi- bility of controlling the crack jumping phenomenon. After being tested, parts of the specimens were cut and observed using an optical microscope to determine the crack path. The results showed that by increasing the flexural stiffness of the crack arms the crack jumping under mode I propagation can be avoided. The fracture toughness values were more affected by the fiber bridging than by the mismatch angles between the layers interfacing the crack plane. The measured effect of fiber bridging is 47% whereas the effect of the mismatch angle is 29%. The optical microscope images show that the delaminations are not a truly interlaminar fractures. Instead, the fiber tearing is more common along the crack propagation path. More investigations are required to understand the phenomenon of crack path and its driving factors in multidirectional laminates.

References

The first author would like to thank the Generalitat de Catalunya for the FI predoctorate grant 2010FI B00756. The authors acknowledge the financial support of the Ministerio de Ciencia e Innovación under the project MAT2009-07918.

References

[1] Robinson P., Song D.Q. A modified DCB specimen for mode I testing of multidirectional laminates. *Journal of Composite Materials*, **26**, pp. 1554–77 (1992).

[2] Hunston D.L., Bascom W.D. Effects of lay-up, temperature and loading rate in double cantilever beam tests of interlaminar crack growth. *Composites Technology Review*, **5**, pp. 118–119 (1982).

[3] Prombut P., Michel L., Lachaud F., Barrau J.J. Delamination of multidirectional composite laminates at 0º/θº ply interfaces. *Engineering Fracture Mechanics*, **73**, pp. 2427–2442 (2006).

[4] Sebaey T.A., Blanco N., Lopes C.S., Costa J. Numerical investigation to prevent crack jumping in double cantilever beam tests of multidirectional composite laminates. *Composites Science and Technology*, **71**, pp. 1587–1592 (2011).

[5] Renart J., Blanco N., Pajares E., Costa J., Lazcano S., Santacruz G. Side Clamped Beam (SCB) hinge system for delamination tests in beam-type composite specimens. *Composites Science and Technology*, **71**, pp. 1023–1029 (2011).

[6] Gong X.J., Hurez A., Verchery G. On the determination of delamination toughness by using multidirectional DCB specimens. *Polymer Testing*, **29**, pp. 658–666 (2010).

[7] Gilchrist M.D., Svensson N. A fractographic analysis of delamination within multidirectional carbon/epoxy laminates. *Composites Science and Technology*, **55**, pp. 195–207 (1995).

[8] Mohamed Rehan M.S., Rousseau J., Gong X.J., Guillaumat L., Ali J.S.M. Effects of fiber orientation of adjacent plies on the mode I crack propagation in a carbon-epoxy laminates. *Procedia Engineering*, **10**, pp. 3179–3184 (2011).

[9] Shokrieh M.M., Heidari-Rarani M. Effect of stacking sequence on R-curve behavior of glass/epoxy DCB laminates with 0º//0º crack interface. *Materials Science and Engineering A*, **529**, pp. 265–269 (2011).

[10] Iwamoto M., Ni Q.Q., Fujiwara T., Kurashiki K. Intralaminar fracture mechanism in unidirectional CFRP composites. Part I : Intralaminar toughness and AE characteristics. *Engineering Fracture Mechanics*, **64**, pp. 721–745 (1999).

[11] de Moura M.F.S.F., Campilho R.D.S.G., Amaro A.M., Reis P.N.B. Interlaminar and intralaminar fracture characterization of composites under mode I loading. *Composite Structures*, **92**, pp. 144–149 (2010).

[12] Hwang J.H., Lee C.S., Hwang W. Effect of crack propagation directions on the interlaminar fracture toughness of carbon /epoxy composite materials. *Applied Composite Materials*, **8**, pp. 411–433 (2001).